

Supporting Information

Jenkitkasemwong et al. 10.1073/pnas.1720739115

SI Methods

Suppression of SLC39A14 Expression in HepG2 Cells and Measurement of Mn Uptake. HepG2 cells were cultured in DMEM with 4.5 g/L glucose, 4 mM L-glutamine, 1 mM sodium pyruvate, 1× minimum Eagle's medium nonessential amino acids (Mediatech), 100 units/mL penicillin, 100 µg/mL streptomycin, and 10% FBS. Cells were maintained at 37 °C in 5% CO₂. HepG2 cells were plated into a six-well plate at 2 × 10⁵ cells per well the day before siRNA transfection. Cells were transfected with 10 nM siRNA targeting SLC39A14 mRNA (SMARTpool: ON-TARGETplus SLC39A14 siRNA; Dharmacon) or negative control siRNA (ON-TARGETplus Nontargeting Pool; Dharmacon) by using Lipofectamine RNAiMAX transfection reagent (Invitrogen). Cells were assayed for Mn uptake after 48 h of transfection. Briefly, cells were washed twice with serum-free medium (SFM) and incubated for 30 min in SFM containing 2% (wt/vol) BSA to deplete cells of transferrin and to block the nonspecific binding at 37 °C. The cells were then incubated with 2 µM [⁵⁴Mn]MnCl₂ in SFM for 1 h at 37 °C, followed by one wash of ice-cold SFM and three washes of an ice-cold chelator solution (0.05% EDTA in PBS) to remove any surface-bound Mn. The cells were lysed in a buffer containing 0.2 M NaOH and 0.2% (wt/vol) SDS. Radioactivity was determined by γ -counting, and protein concentration was determined colorimetrically by using the RC DC Protein Assay (Bio-Rad).

Western Blot Analysis for DMT1, SLC39A8, TfR1, and SLC39A14. Mouse liver lysates were prepared by homogenizing liver samples in ice-cold radioimmunoprecipitation assay (RIPA) buffer containing 1× Complete Mini Protease Inhibitor Mixture (Roche). The lysates were sonicated on ice and centrifuged at 10,000 × *g* for 15 min at 4 °C to remove nuclei and cell debris. Supernatants were collected for subsequent analyses or stored at -80 °C. For the siRNA experiment in HepG2 cells, cells were lysed in RIPA buffer containing 1× Complete Mini Protease Inhibitor Mixture. Protein concentrations of samples were determined by using the RC DC Protein Assay. Samples were mixed with Laemmli sample buffer and incubated for 30 min at 37 °C for DMT1 detection, boiled for 5 min at 98 °C for TfR1 detection, or without heating for SLC39A14 detection. For SLC39A8 detection, liver samples were deglycosylated by treatment with PNGase F (catalog no. P0704; New England BioLabs) for 1 h at 37 °C before mixing with Laemmli sample buffer. Samples were then electrophoretically separated on a 7.5% SDS-polyacrylamide gel, transferred to nitrocellulose, and incubated for 1 h in blocking buffer [5% nonfat dry milk in Tris-buffered saline-Tween 20 (TBS-T)]. Blots were then incubated

overnight at 4 °C in blocking buffer containing either a rabbit anti-DMT1 antibody (1:2,000, kind gift from Francois Canonne-Hergaux, INSERM, Toulouse, France), a mouse anti-TfR1 antibody (1:1,000, catalog no. 13-6890; Life Technologies), a rabbit anti-SLC39A14 antibody (1 µg/mL, HPA-016508; Sigma), or a rabbit anti-SLC39A8 antibody [2 µg/mL (1)]. After four washes in TBS-T, blots were incubated for 40 min with a horseradish peroxidase (HRP)-conjugated donkey anti-rabbit IgG secondary antibody (1:2,000, catalog no. NA9340V; GE Healthcare) or an HRP-conjugated goat anti-mouse IgG secondary antibody (1:1,000, catalog no. 32430; Invitrogen). Blots were then washed with TBS-T and TBS, and immunoreactivity was visualized by using enhanced chemiluminescence (SuperSignal West Pico or West Femto; Pierce) and the FluorChem E digital darkroom (ProteinSimple). To indicate lane loading, blots were stripped and reprobed with a rabbit anti-SR-B1 antibody (1:2,000; catalog no. NB400-104; Novus Biologicals) followed by an HRP-conjugated donkey anti-rabbit IgG secondary antibody.

Liver-specific DMT1 knockout (*Dmt1^{liv/liv}*) liver (2) was used as a negative control for DMT1. Liver-specific SLC39A8 knockout (*Slc39a8^{liv/liv}*) liver was used as a negative control for SLC39A8. *Slc39a8^{liv/liv}* mice were generated from conditional-ready *Slc39a8^{fllox/fllox}* mice that we derived from *Slc39a8^{fllox-neo/+}* mice [C57BL/6NTac-Slc39a8tm1a(EUCOMM)Wtsi/Cnrm; European Mouse Mutant Archive].

Initial Assessment of Motor Phenotype. Unless otherwise noted, all housing and experimental conditions for the mice used for our supplemental behavioral data were the same as stated in *Methods*. **Mice.** Mice maintained on a B6;129S genetic background and on a congenic 129S6 genetic background were used for the initial behavioral analysis. The mice were bred in-house in the Animal Care facility at the University of Florida, Gainesville.

Experimental design. The mice were transferred to the behavioral laboratory at the age of 8 wk. Their body weight was recorded upon arrival, and, afterward, the mice were weighed repeatedly up to the age of 52 wk, when the tests were concluded. During all experimental manipulations, the mice were handled using the hand-cupping method. The behavioral tests were administered sequentially with a SHIRPA overall screen first, followed by the pole test (~26 wk), grip test, beam-traversing test, and rotarod test. The cohort of *Slc39a14^{-/-}* mice maintained on B6;129 background was tested in this battery of tests at 12 and 52 wk of age following a longitudinal design, whereas the cohort maintained on the congenic 129S background was tested at 13 mo in a cross-sectional design.

1. Wang CY, et al. (2012) ZIP8 is an iron and zinc transporter whose cell-surface expression is up-regulated by cellular iron loading. *J Biol Chem* 287:34032–34043.
2. Wang CY, Knutson MD (2013) Hepatocyte divalent metal-ion transporter-1 is dispensable for hepatic iron accumulation and non-transferrin-bound iron uptake in mice. *Hepatology* 58:788–798.

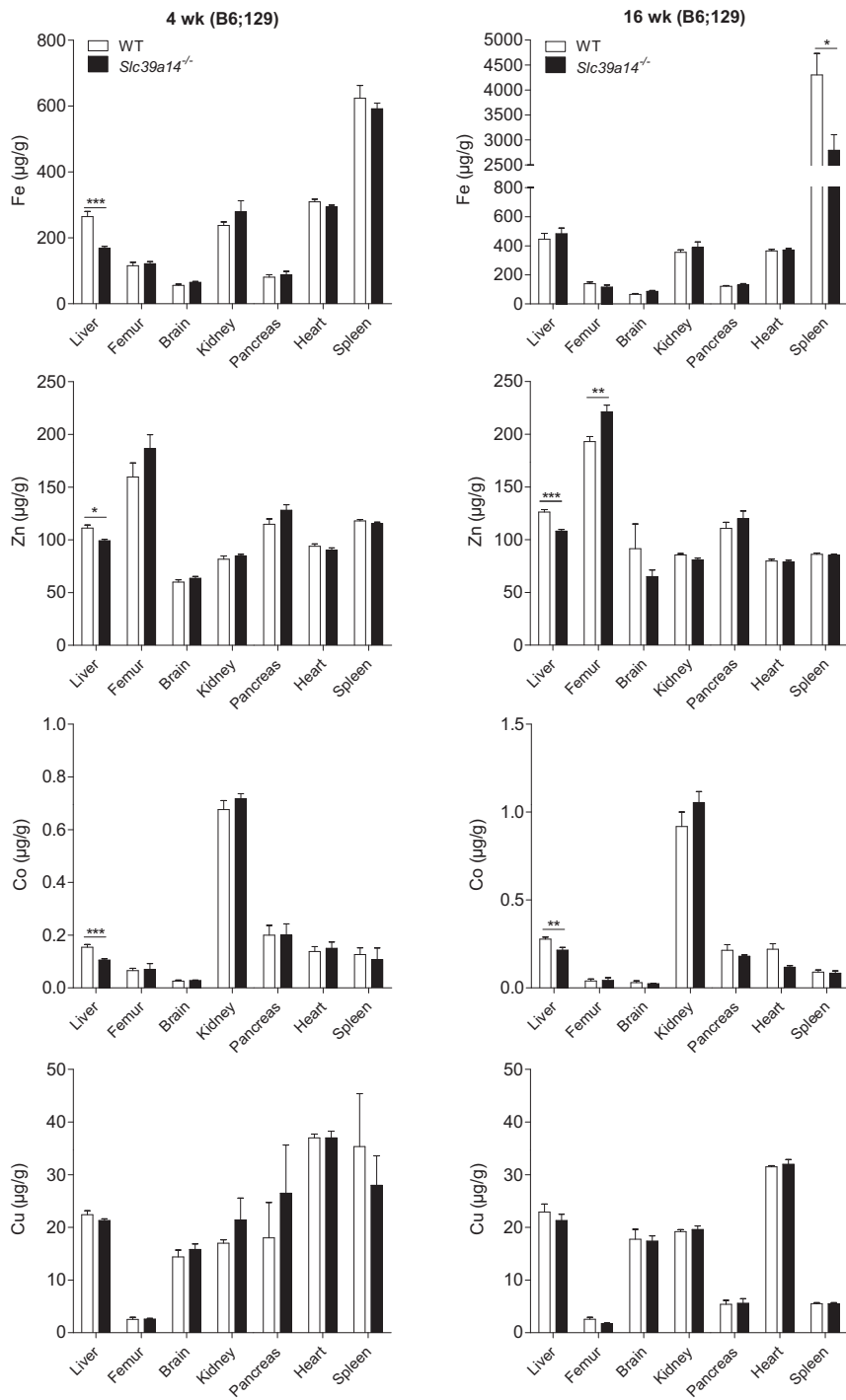


Fig. S1. Tissue concentrations of iron, zinc, cobalt, and copper in WT and *Slc39a14*^{-/-} mice. Metal concentrations in various tissues of *Slc39a14*^{-/-} mice and WT littermate controls were determined by using ICP-MS. Tissues were from mixed-background B6;129 male and female mice at 4 and 16 wk of age ($n = 4-10$ per genotype). Mn concentrations are shown in Fig. 1 A and B. Data represent mean \pm SEM. * $P < 0.05$; ** $P < 0.01$; *** $P < 0.001$.

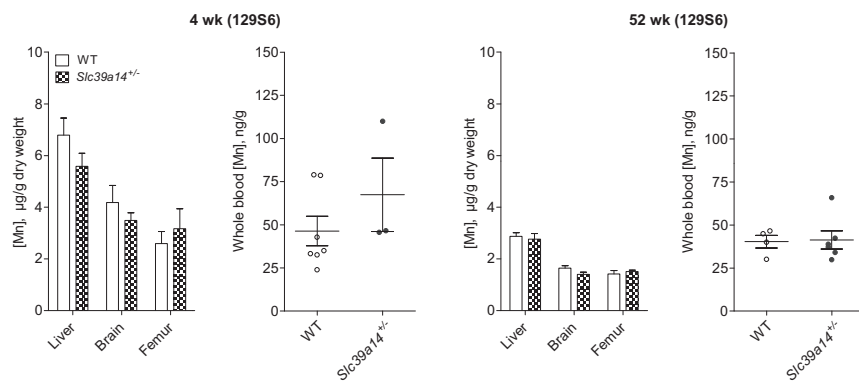


Fig. S2. Tissue Mn concentrations are not altered in hemizygous *Slc39a14*^{+/-} mice. Mn concentrations in *Slc39a14*^{+/-} mice and WT littermate controls were determined by using ICP-MS. The liver, brain, femur ($n = 4\text{--}6$ per genotype) and whole blood ($n = 3\text{--}7$ per genotype) were from congenic 129S6 male and female mice at 4 and 52 wk of age. Data represent mean \pm SEM.

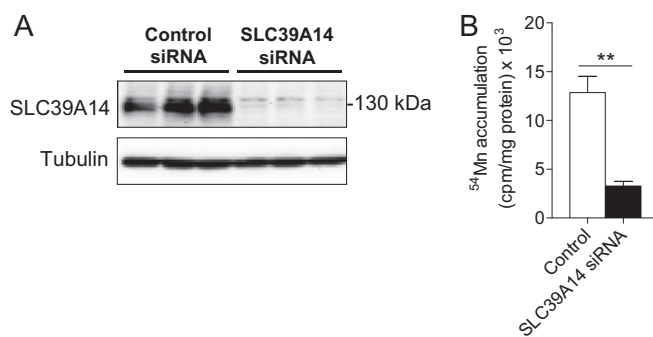


Fig. S3. Knockdown of SLC39A14 decreases Mn accumulation in HepG2 cells. (A) Western blot analysis of ZIP14 in lysates from HepG2 cells treated with control siRNA or siRNA targeting SLC39A14. Results shown are representative of three independent experiments with similar results. (B) Cellular accumulation of ⁵⁴Mn in HepG2 cells treated with control siRNA or siRNA targeting SLC39A14. Cells were incubated with 2 mM [⁵⁴Mn]MnCl₂ for 1 h, and cellular accumulation of ⁵⁴Mn was measured by γ -counting. Data represent mean \pm SEM of three independent experiments. ** $P < 0.01$.

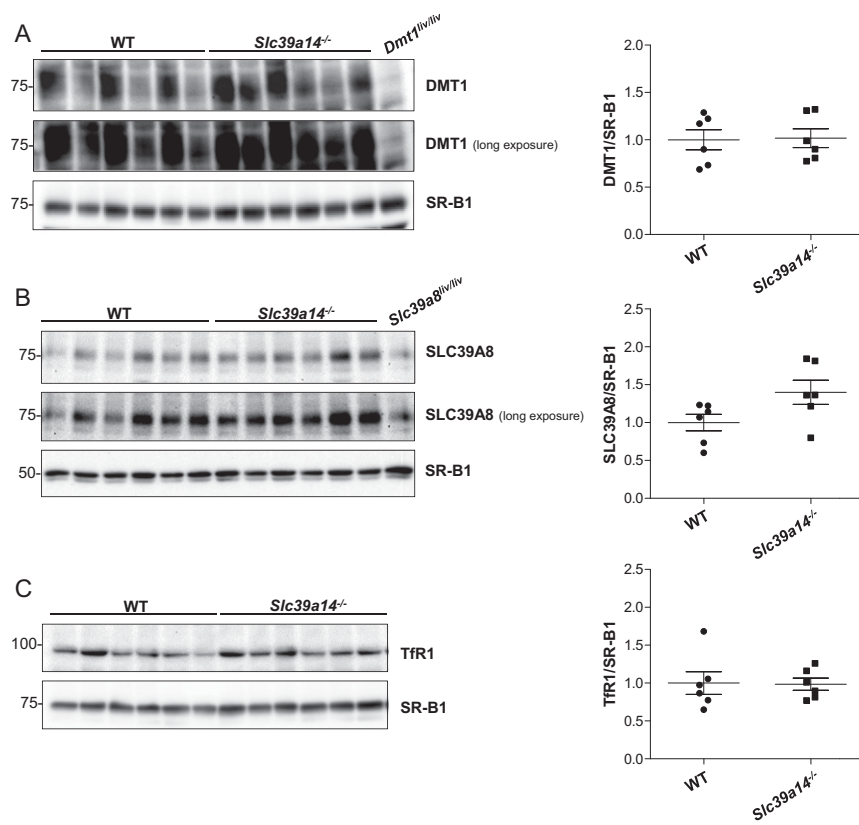


Fig. S4. Hepatic DMT1, SLC39A8, and Tfr1 levels in *Slc39a14*^{-/-} mice at 16 wk of age. (Left) Western blot analyses of DMT1 (A), SLC39A8 (B), and Tfr1 (C) in total liver lysates from WT and *Slc39a14*^{-/-} mice ($n = 6$ per group, $n = 3$ male, $n = 3$ female from left to right) at 16 wk of age. (A) Liver-specific DMT1 knockout (*Dmt1*^{liv/liv}) liver was used as a negative control for DMT1 (far right lane). (B) Liver-specific SLC39A8 knockout (*Slc39a8*^{liv/liv}) liver was used as a negative control for SLC39A8 (far right lane). Data shown are representative of at least two independent experiments with similar results. (Right) Densitometric analyses of protein levels as normalized to the lane loading control scavenger receptor-B1 (SR-B1) are shown. Data represent mean \pm SEM and were analyzed by using an unpaired Student's t test.

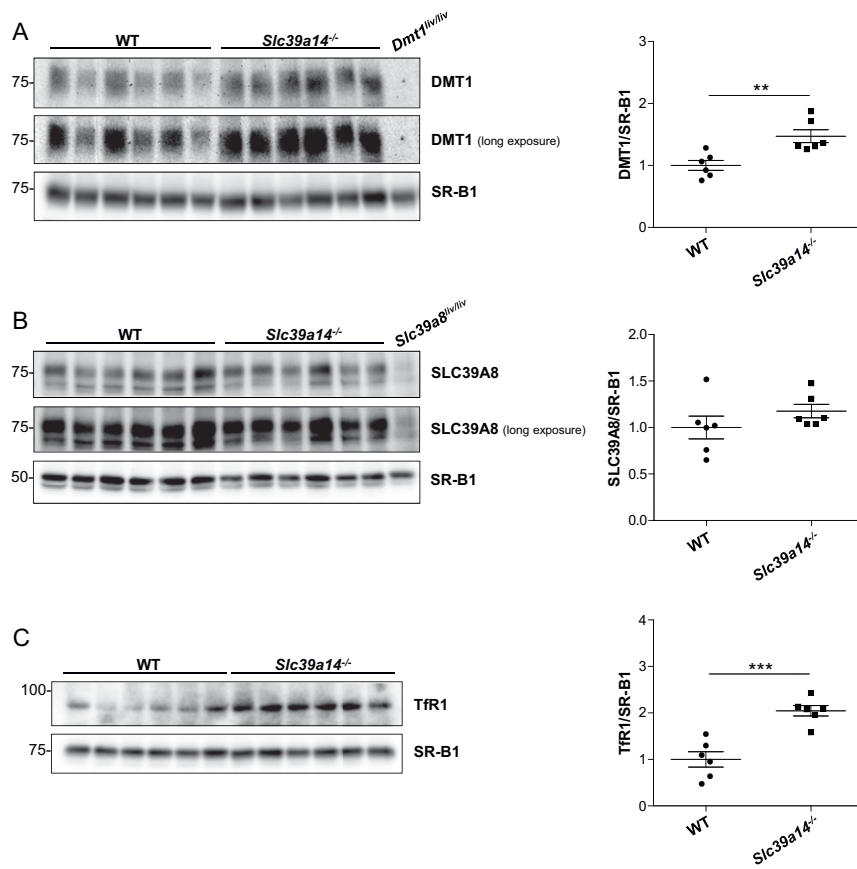


Fig. S5. Hepatic DMT1, SLC39A8, and Tfr1 levels in *Slc39a14^{-/-}* mice at 4 wk of age. (Left) Western blot analyses of DMT1 (A), SLC39A8 (B), and Tfr1 (C) in total liver lysates from WT and *Slc39a14^{-/-}* mice ($n = 6$ per group, $n = 3$ male, $n = 3$ female from left to right) at 4 wk of age. (A) Liver-specific DMT1 knockout (*Dmt1^{liver/liver}*) liver was used as a negative control for DMT1 (far right lane). (B) Liver-specific SLC39A8 knockout (*Slc39a8^{liver/liver}*) liver was used as a negative control for SLC39A8 (far right lane). Data shown are representative of at least two independent experiments with similar results. (Right) Densitometric analyses of protein levels as normalized to the lane loading control scavenger receptor-B1 (SR-B1) are shown. Data represent mean \pm SEM and were analyzed by using an unpaired Student's t test. ** $P < 0.01$; *** $P < 0.001$.

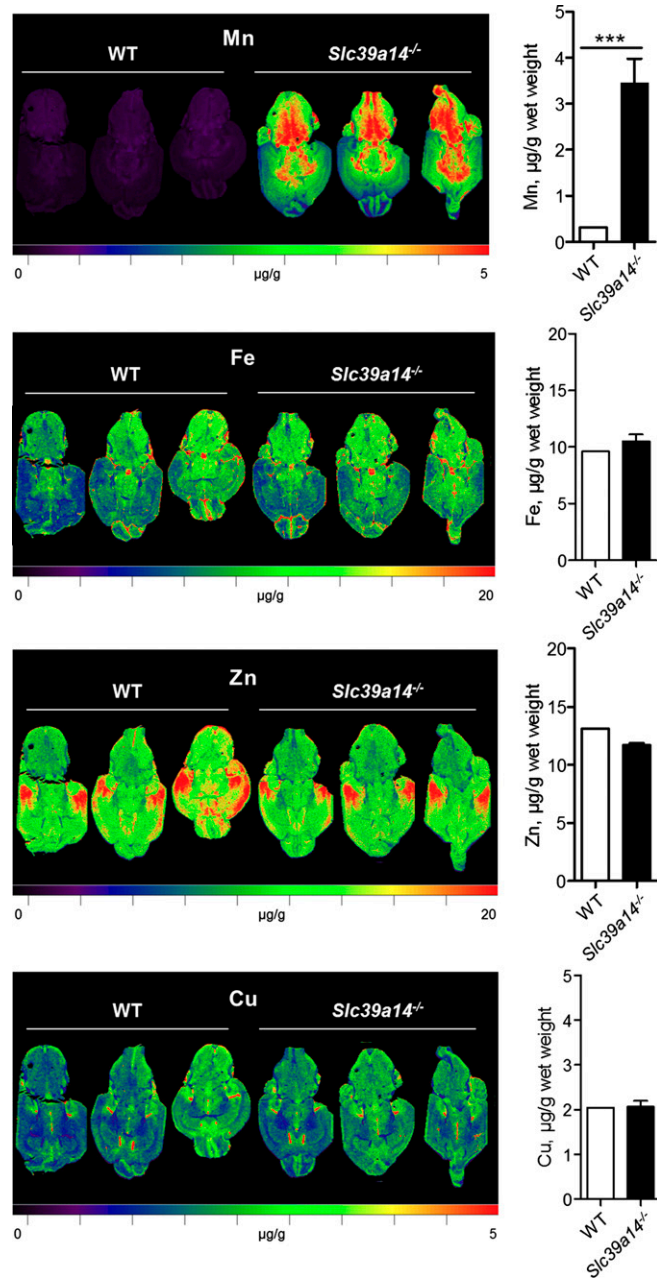


Fig. S6. Regional distribution and quantification of Mn, Fe, Zn, and Cu in *Slc39a14*^{-/-} mouse brain. (Left) Horizontal cryosections from WT [$n = 3$, $n = 1$ male (M), $n = 2$ female (F)] and *Slc39a14*^{-/-} ($n = 3$, $n = 1$ M, $n = 2$ F) mice at 3 wk of age were subjected to LA-ICP-MS imaging. Metal concentrations are indicated by a color scale, with maximum threshold indicated by red. (Right) Bar graphs at Right indicate average metal concentrations (mean \pm SD) of the entire cryosection. *** $P < 0.001$.

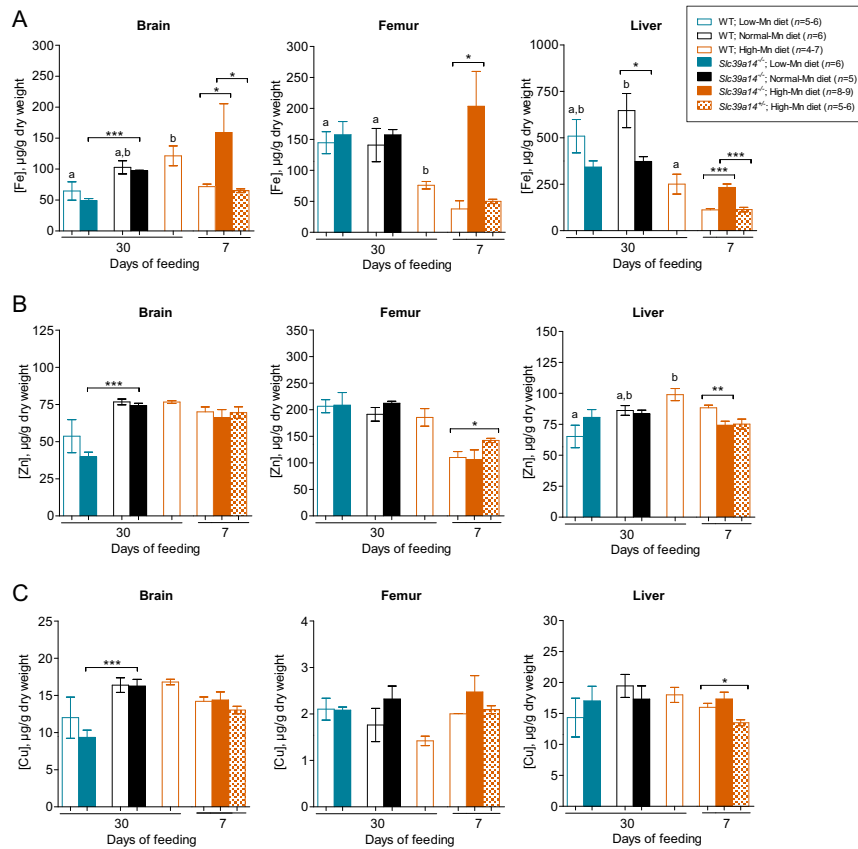


Fig. S7. Tissue iron, zinc, and copper concentrations in WT and *Slc39a14*^{-/-} mice used for the Mn feeding study (Fig. 5). Metal concentrations in various tissues from *Slc39a14*^{-/-} mice and WT littermate controls were determined by using ICP-MS. (A–C) Iron, zinc, and copper concentrations in the brain, femur, and liver of mice fed the low-Mn diet [WT: $n = 5-6$, $n = 3$ male (M), $n = 2-3$ female (F); *Slc39a14*^{-/-}: $n = 6$, $n = 3$ M, $n = 3$ F], normal-Mn diet (WT: $n = 6$, $n = 3$ M, $n = 3$ F; *Slc39a14*^{-/-}: $n = 5$, $n = 2$ M, $n = 3$ F), or high-Mn diet (WT: $n = 4-5$, $n = 2$ M, $n = 2-3$ F) for 30 d (or only 7 d for *Slc39a14*^{-/-} mice fed the high-Mn diet: $n = 8-9$, $n = 6$ M, $n = 2-3$ F). For comparison, tissues from WT ($n = 6-7$, $n = 2-3$ M, $n = 3-5$ F) and hemizygous *Slc39a14*^{+/-} ($n = 5-6$, $n = 2-3$ M, $n = 3$ F) mice were also analyzed after only 7 d of feeding. Data represent mean \pm SEM and were statistically analyzed by using either an unpaired Student's *t* test or one-way ANOVA. * $P < 0.05$; ** $P < 0.01$; *** $P < 0.001$. Means without a common superscript letter differ significantly ($P < 0.05$).

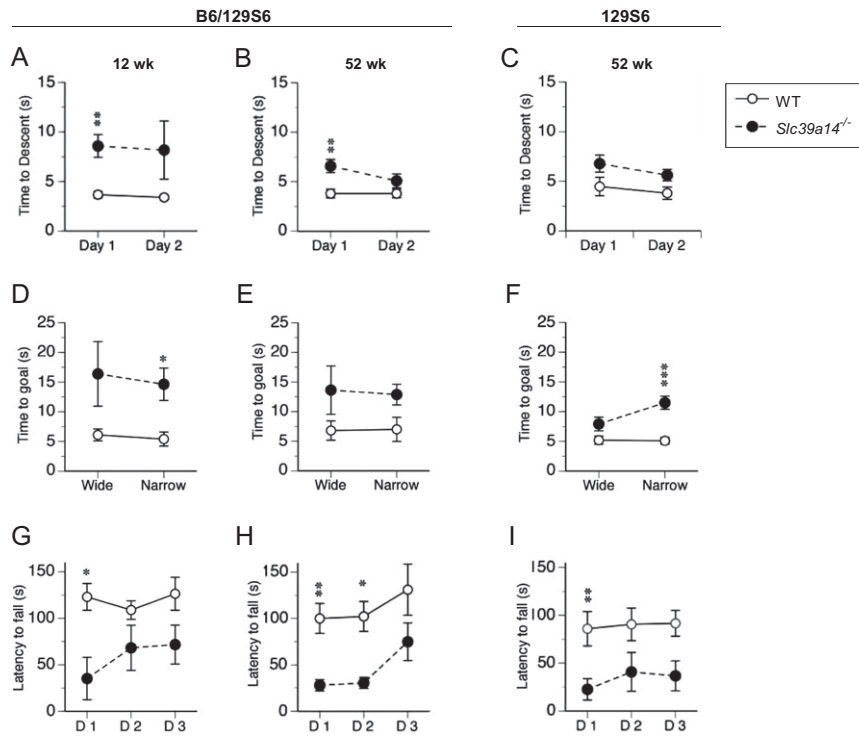


Fig. S8. *Slc39a14*^{-/-} mice display behavioral motor impairments. Two cohorts of mice, maintained on a hybrid B6;129 background and an incipient congenic 129S6 genetic background, were tested in a battery of locomotor tests, including the pole test (A–C), beam-traversing test (D–F), and rotarod test (G–I). The B6;129 mice [WT: $n = 5$, $n = 3$ male (M), $n = 2$ female (F); *Slc39a14*^{-/-}: $n = 4$, $n = 2$ M, $n = 2$ F] were tested at 12 and 52 wk of age following a longitudinal design; the 129S6 mice (WT, $n = 5$, $n = 3$ M, $n = 2$ F; *Slc39a14*^{-/-}: $n = 6$, $n = 3$ M, $n = 3$ F) were tested at 52 wk of age following a cross-sectional design. *Slc39a14*^{-/-} mice displayed consistent age- and background-independent longer times to descend a 50-cm vertical pole (A–C), longer times to traverse elevated horizontal beams [2.5 cm (wide) and 1.7 cm (narrow)] (D–F), and shorter latencies to fall on an accelerated (4–40 rpm) 5-min rotarod test (G–I). D1, D2, and D3 denote day 1, day 2, and day 3, respectively. Data represent mean \pm SEM. * $P < 0.05$; ** $P < 0.01$; *** $P < 0.001$.

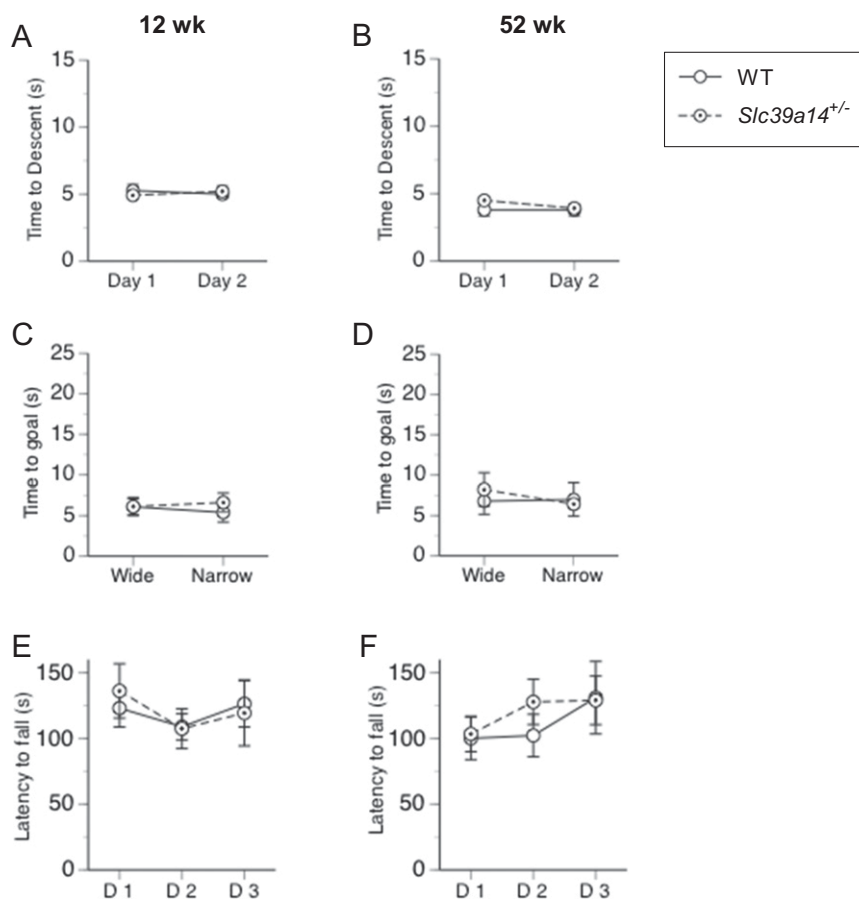


Fig. 59. Lack of motor impairment in *Slc39a14*^{+/-} hemizygous mice. Cohorts of *Slc39a14*^{+/-} mice [$n = 8$, $n = 4$ male (M), $n = 4$ female (F)] and their control WT littermates ($n = 5$, $n = 3$ M, $n = 2$ F), maintained on a hybrid B6;129S background, were tested in a battery of locomotor tests, including the pole test (A and B), beam-traversing test (C and D), and rotarod test (E and F). The mice were tested at 12 wk (A, C, and E) and 52 wk (B, D, and F) of age following a longitudinal design. *Slc39a14*^{+/-} mice and their control littermates displayed similar times to descend a 50-cm vertical pole (A and B), similar times to traverse elevated horizontal beams [2.5 cm (wide) and 1.7 cm (narrow)] (C and D), and similar latencies to fall on an accelerated (4–40 rpm) 5-min rotarod test (E and F). D1, D2, and D3 denote day 1, day 2, and day 3, respectively. Data represent mean \pm SEM.

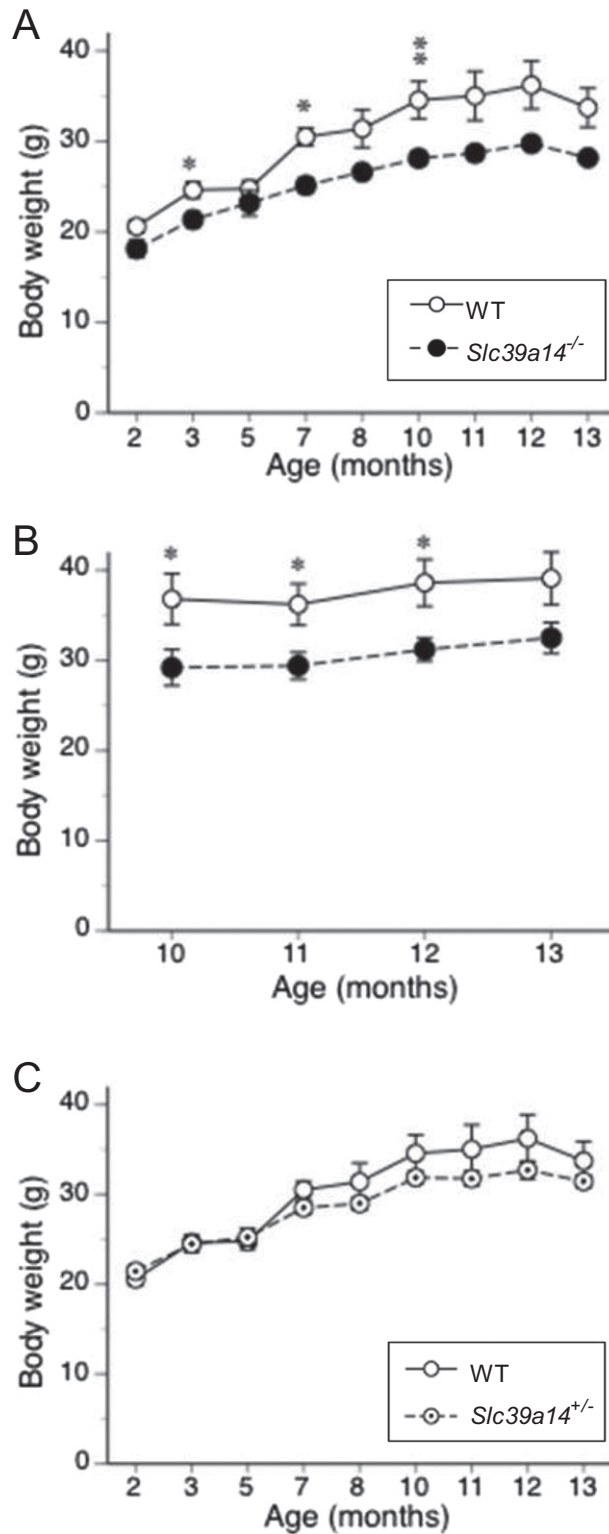


Fig. S10. *Slc39a14^{-/-}* but not *Slc39a14^{+/-}* mice exhibit lower body weights. (A) *Slc39a14^{-/-}* mice [$n = 4$, $n = 2$ male (M), $n = 2$ female (F)] and their control WT littermates ($n = 5$, $n = 3$ M, $n = 2$ F), maintained on a B6;129S genetic background, were weighed between 8 and 52 wk of age. (B) *Slc39a14^{-/-}* mice ($n = 6$, $n = 3$ M, $n = 3$ F) and their WT littermates ($n = 5$, $n = 3$ M, $n = 2$), maintained on a 129S6 incipient congenic genetic background, were weighed between 30 and 52 wk of age. (C) Hemizygous *Slc39a14^{+/-}* mice ($n = 8$, $n = 4$ M, $n = 4$ F) and their control WT littermates ($n = 5$, $n = 3$ M, $n = 2$ F), maintained on a B6;129S genetic background, were weighed between 8 and 52 wk of age. Data represent mean \pm SEM. * $P < 0.05$; ** $P < 0.01$.

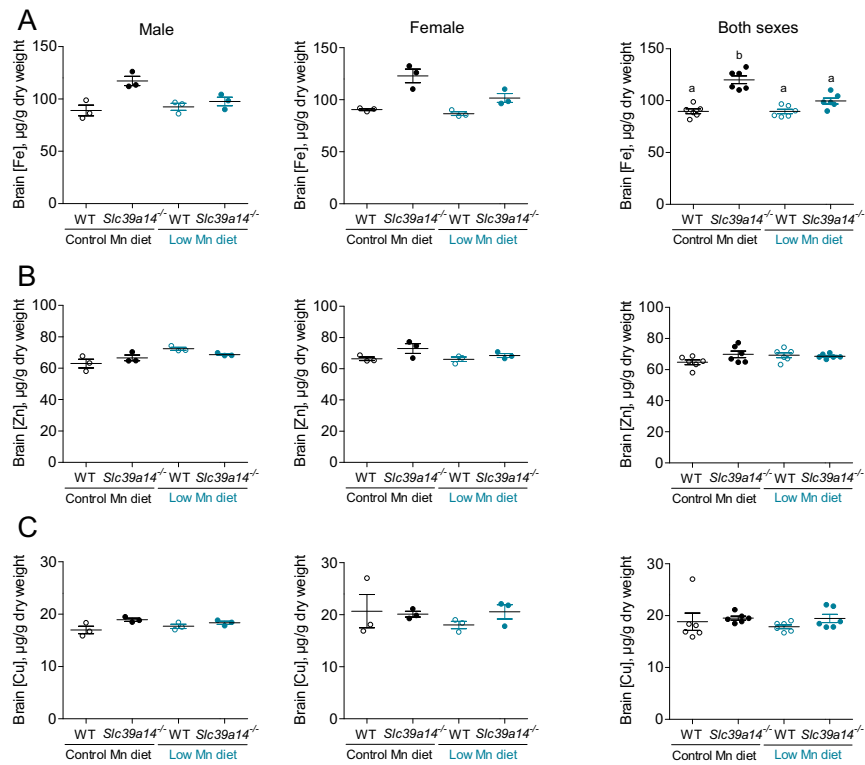


Fig. S11. Brain iron, zinc, and copper in WT and *Slc39a14*^{-/-} mice used for the behavioral evaluation study (Fig. 6). (A–C) Iron, zinc, and copper concentrations in the brain of ~15-wk-old male (Left) and female (Center) WT and *Slc39a14*^{-/-} mice ($n = 3$ per group per sex) maintained on the control-Mn diet or the low-Mn diet from weaning. Data represent mean \pm SEM. (Right) Combined data from both sexes (far right graphs) were analyzed by using one-way ANOVA. Means without a common superscript letter differ significantly ($P < 0.0001$).